HISTORICAL PERSPECTIVE

A Reflection on the Evolution of Antibody-Based Therapies in Oncology: Trastuzumab as an Exemplar—Commentary on Dijkers *et al*.

Sarah A. Holstein*

Since the first description of hybridoma cells capable of producing monoclonal antibodies (mAbs) 50 years ago, remarkable progress has been made in the development of antibody-based therapies in oncology. Featured in this issue of CPT is an article first published in 2010 describing ^{89}Zr-trastuzumab for immuno-positron emission tomography (PET) imaging. This commentary places the development of HER2-targeted agents within the greater context of antibody-based development in oncology and the accompanying evolution of clinical pharmacology.

The year 2025 marks the 50th anniversary of Köhler and Milstein's publication reporting the generation of hybridoma cell lines capable of producing mAb.[1] Not only has this discovery enabled scientific progress across the spectrum of biomedical research, but the impact on clinical pharmacology and therapeutics has been remarkable. In 1980, Nadler et al. published a case report detailing the transient activity of a murine mAb targeting a lymphoma-associated antigen.[2] Antibody-based therapies have subsequently evolved from murine mAbs to chimeric mAbs to humanized mAbs to fully human mAbs, radiolabeled antibodies, antibody-drug conjugates (ADCs), bispecific T-cell engagers (BiTEs) and bispecific antibodies (BsAbs), amongst others. While many of the mAbs have targeted tumor-specific antigens, others have been more directly immunomodulatory in nature (e.g., checkpoint inhibitors), yielding impressive results in previously difficult-to-treat malignancies (e.g., melanoma, renal cell carcinoma). A 2022 publication reported that the Umabs Antibody Therapies Database listed 162 antibody therapies that had been approved by at least one regulatory agency (not including biosimilar, diagnostic and veterinary antibodies).[3] These 162 antibody therapies encompassed 91 drug targets and included 115 canonical antibodies, 14 ADCs, 7 BsAbs, 8 antibody fragments, 3 radiolabeled antibodies, 1 antibody-conjugate immunotoxin, 2 immunoconjugates, and 12 Fc-Fusion proteins.[3] The field of cancer has been most prominently impacted by the development of mAb-based therapies, with 66 antibody therapeutics granted a first approval for a cancer indication in the United States or the European Union between 1997 and 2024.[4] Not included in these totals are therapies such as chimeric antigen receptor (CAR) T-cell products which include an antibody fragment in the CAR construct. **Figure 1** highlights some of the major events over the past 50 years that have transformed the cancer therapeutic landscape from an antibody-based perspective.

The first humanized mAb to receive FDA approval for a solid tumor indication was trastuzumab in 1998. Trastuzumab targets the extracellular domain of human epidermal growth factor receptor 2 protein (HER-2) and is thought to induce cell death through multiple mechanisms of action, including attenuation of signal transduction pathways downstream of HER2, induction of antibody-dependent cellular cytotoxicity (ADCC) and prevention of HER2 shedding. Trastuzumab was first approved for the treatment of HER2-positive metastatic breast cancer and then later approved in the adjuvant setting. There has subsequently been a slew of HER2-targeting antibody-based therapies approved for the treatment of HER2-positive breast cancer, including another mAb (pertuzumab, which binds to a different extracellular domain of HER2, blocking ligand-dependent heterodimerization with HER1, HER3, and HER4, and is only approved in combination with trastuzumab), a chimeric Fc-engineered mAb (margetuximab, which induces ADCC and is approved for use in combination with chemotherapy) and two ADCs (Fam-trastuzumab deruxtecan (T-DXd) and Ado-trastuzumab emtansine (T-DM1)). In addition, multiple tyrosine kinase

Department of Internal Medicine, University of Nebraska Medical Center, Omaha, Nebraska, USA. *Correspondence: Sarah A. Holstein (sarah.holstein@unmc.edu)

Received January 20, 2025; accepted March 10, 2025. doi:10.1002/cpt.3651

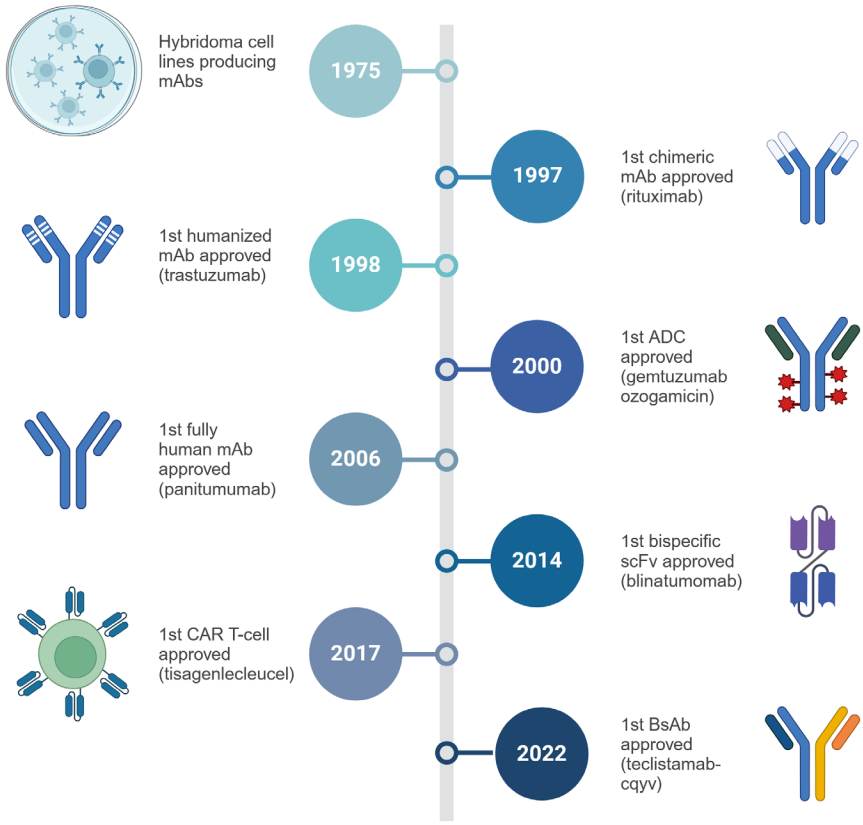

Figure 1 Major events over the past 50 years in the development of antibody-based therapies for oncology, including first-in-class approvals by the FDA. ADC, antibody-drug conjugate; BsAb, bispecific antibody; CAR, chimeric antigen receptor; mAb, monoclonal antibody; scFv, single-chain variable fragment.

inhibitors (TKIs) have been approved: lapatinib targets EGF1 and HER2, neratinib is an irreversible pan-HER inhibitor, and tucatinib targets HER2.

There has also been significant interest in the development of radiolabeled derivatives of trastuzumab, representative of the emerging field of radiotheranostics.[5] The article chosen to highlight the 2010–2019 era of *Clinical Pharmacology & Therapeutics* was first published in 2010 by Dijkers et al.[6] This manuscript reported the results of a feasibility study in which patients with HER2-positive metastatic breast cancer received a dose of ^{89}Zr-trastuzumab followed by PET imaging. This built upon prior work demonstrating that ^{111}In-trastuzumab could identify HER2-positive lesions that were previously undetected using conventional imaging.[7] The advent of ^{89}Zr-labeled antibodies for clinical immunoPET imaging enabled the use of a positron-emitting radiolabel with a longer half-life (78.4 hours), permitting imaging up to 1 week after injection. Dijkers et al. demonstrated accumulation of the ^{89}Zr-trastuzumab in liver, lung, bone, and brain metastases. Although not all of the previously known lesions were identified with ^{89}Zr-trastuzumab, in some cases, immunoPET identified new lesions.[6] While immunoPET imaging with ^{89}Zr-trastuzumab has not yet entered into clinical practice, research in this space has continued. Bensch et al. explored whether ^{89}Zr-trastuzumab PET could be used to support clinical decision-making in cases where there was uncertainty about the HER2 status in patients with breast cancer.[8] Although the outcomes of this study were subjective in that they were primarily related to whether treating physicians thought the imaging results improved diagnostic understanding or informed choice of therapy, this work did support the hypothesis that ^{89}Zr-trastuzumab PET could be used as a diagnostic tool. Other groups have explored alternative radiolabels or mAbs for HER2-targeted immunoPET applications, including ^{89}Zr-pertuzumab[9] and ^{64}Cu-DOTA-trastuzumab.[10] IMPACT-MBC (NCT01957332), a prospective multicenter observational cohort study, was initiated in 2013 in the Netherlands and is anticipated to be completed in 2027. The primary objective of this study is to evaluate the clinical utility of experimental PET scans (including ^{89}Zr-trastuzumab PET) in the setting of metastatic breast cancer at first presentation and will hopefully shed light on whether the use of ^{89}Zr-trastuzumab PET should be integrated into the care of patients with HER2-positive disease.

In many ways, trastuzumab and the subsequent development of other HER2-targeting antibody-based therapies are illustrative of the field as a whole. What began as single-agent mAb therapy for metastatic HER2-positive breast cancer evolved into combination-based therapies (e.g., with traditional cytotoxic agents, hormonal agents, other anti-HER2 mAb, or anti-HER2 TKIs). From there came the understanding that therapies could be target-specific, but tissue agnostic and trastuzumab is now approved for the treatment of other HER2-positive malignancies such as colorectal cancer, endometrial cancer, biliary cancer, and gastric cancer. The development of mAbs linked to toxins (i.e., the ADCs) provided an innovative way of selectively delivering cytotoxic therapy to tumor cells of interest. In fact, the first ADC to gain FDA approval for a solid tumor indication was the trastuzumab-based T-DM1 in 2013, which retains the trastuzumab-mediated actions against HER2-expressing cells while also enabling targeted delivery of the anti-microtubule agent emtansine. The first HER2 × HER3 BsAb (zenocutuzumab) was approved for pancreatic adenocarcinoma and non-small cell lung cancer harboring neuregulin 1 (NRG1) gene fusions in 2024. This agent has been referred to as having a "dock and block" mechanism whereby the HER2-targeting arm docks the antibody, providing a high local concentration and positioning the HER3-targeting arm to block binding of NRG1 to HER3, resulting in the prevention of phosphorylation of the cytoplasmic domain of HER3 and downstream signaling.[11] CAR T-cell therapies, which rely on the external domain

of the construct containing a scFv domain to recognize the target tumor antigen of interest, have proven to be truly groundbreaking for a variety of hematological malignancies. The number of CAR T trials for solid tumors is continuing to grow. While an initial attempt at a HER2 CAR T based on trastuzumab resulted in the study terminating after the first patient experienced respiratory distress shortly after infusion resulting in death within 1 week,[12] alternative approaches such as TRAIL-R2 and HER2 bispecific CAR T-cells are being pursued (NCT06251544).

The incredible therapeutic successes achieved during the evolution of antibody-based therapies in oncology over the last several decades have brought with them a myriad of new challenges for the field of clinical pharmacology. It became evident that traditional pharmacokinetic (PK) modeling and dose–response determinations that were established in the era of small molecule drugs required adjustments in the era of antibody-based therapies. Target engagements now need to be considered in the setting of multiple targets on different cell types (e.g., the tumor antigen on tumor cells and CD3 on T cells), and traditional maximum tolerated dose determinations are no longer appropriate (as recognized by the FDA's Project Optimus initiative). Recent perspectives for bispecific-based therapies[13,14] and ADCs[15] outline the complexities associated with determining first-in-human dosing, assessment of safety, selection of recommended phase 2 dose, evaluation of immunogenicity, and establishment of appropriate biomarkers. The biosimilar market is a burgeoning market (e.g., there are currently six trastuzumab biosimilars available in the United States) and with that has come new regulatory challenges for the field.[16] Molecularly targeted therapies have enabled the development of biomarker-driven clinical trials and approvals.[17,18] Furthermore, quantitative systems pharmacology has risen to the challenge of integrating virtual patients and trials into the development platforms of immuno-oncology therapies.[19]

In conclusion, the identification of HER2 as a potential therapeutic target for breast cancer, with the subsequent journey from trastuzumab to HER2-targeting tyrosine kinase inhibitors, radiolabeled antibodies, ADCs, BsAbs, and CAR T cells, is illustrative of the remarkable progress that has been achieved in cancer therapy, particularly with respect to antibody-based therapies. Currently, the armamentarium for nearly all malignancies includes therapeutic options derived from antibody-based therapies. Along the way, the contributions of clinical pharmacology in establishing new frameworks for PK-PD determinations, population PK modeling, quantitative systems pharmacology, and trial design have been instrumental to therapeutic successes. The further expansion of molecular subtyping of malignancies, development of personalized therapies, improved understanding of mechanisms of resistance to immuno-oncology therapies, and future breakthroughs in bioengineering of antibody- and cellular-based therapies ensure that those involved in clinical pharmacology research will remain at the forefront of discovery.

FUNDING
No funding was received for this work.

DISCLOSURES
SAH has served as a consultant for Janssen, Sanofi, and Takeda (not related to this work). As an Associate Editor for *Clinical Pharmacology & Therapeutics*, Sarah A. Holstein was not involved in the review or decision process for this paper.

1. Kohler, G. & Milstein, C. Continuous cultures of fused cells secreting antibody of predefined specificity. *Nature* **256**, 495–497 (1975).
2. Nadler, L.M. *et al*. Serotherapy of a patient with a monoclonal antibody directed against a human lymphoma-associated antigen. *Cancer Res.* **40**, 3147–3154 (1980).
3. Lyu, X. *et al*. The global landscape of approved antibody therapies. *Antib Ther.* **5**, 233–257 (2022).
4. The Antibody Society. Therapeutic monoclonal antibodies approved or in regulatory review <www.antibodysociety.org/antibody-therapeutics-product-data> (2025) Accessed January 15 2025.
5. Te Beek, E.T., Burggraaf, J., Teunissen, J.J.M. & Vriens, D. Clinical pharmacology of Radiotheranostics in oncology. *Clin. Pharmacol. Ther.* **113**, 260–274 (2023).
6. Dijkers, E.C. *et al*. Biodistribution of 89Zr-trastuzumab and PET imaging of HER2-positive lesions in patients with metastatic breast cancer. *Clin. Pharmacol. Ther.* **87**, 586–592 (2010).
7. Perik, P.J. *et al*. Indium-111-labeled trastuzumab scintigraphy in patients with human epidermal growth factor receptor 2-positive metastatic breast cancer. *J. Clin. Oncol.* **24**, 2276–2282 (2006).
8. Bensch, F. *et al*. (89)Zr-trastuzumab PET supports clinical decision making in breast cancer patients, when HER2 status cannot be determined by standard work up. *Eur. J. Nucl. Med. Mol. Imaging* **45**, 2300–2306 (2018).
9. Ulaner, G.A. *et al*. First-in-human human epidermal growth factor receptor 2-targeted imaging using (89) Zr-Pertuzumab PET/CT: dosimetry and clinical application in patients with breast cancer. *J. Nucl. Med.* **59**, 900–906 (2018).
10. Tamura, K. *et al*. 64Cu-DOTA-trastuzumab PET imaging in patients with HER2-positive breast cancer. *J. Nucl. Med.* **54**, 1869–1875 (2013).
11. Geuijen, C.A.W. *et al*. Unbiased combinatorial screening identifies a bispecific IgG1 that potently inhibits HER3 signaling via HER2-guided ligand blockade. *Cancer Cell* **33**, 922–936.e10 (2018).
12. Morgan, R.A., Yang, J.C., Kitano, M., Dudley, M.E., Laurencot, C.M. & Rosenberg, S.A. Case report of a serious adverse event following the administration of T cells transduced with a chimeric antigen receptor recognizing ERBB2. *Mol. Ther.* **18**, 843–851 (2010).
13. Nagaraja Shastri, P. *et al*. Industry perspective on first-in-human and clinical pharmacology strategies to support clinical development of T-cell engaging bispecific antibodies for cancer therapy. *Clin. Pharmacol. Ther.* **117**, 34–55 (2025).
14. Lim, K., Zhu, X.S., Zhou, D., Ren, S. & Phipps, A. Clinical pharmacology strategies for bispecific antibody development: learnings from FDA-approved bispecific antibodies in oncology. *Clin. Pharmacol. Ther.* **116**, 315–327 (2024).
15. Liao, M.Z. *et al*. Model-informed therapeutic dose optimization strategies for antibody-drug conjugates in oncology: what can we learn from US Food and Drug Administration-approved antibody-drug conjugates? *Clin. Pharmacol. Ther.* **110**, 1216–1230 (2021).

16. Guillen, E., Ekman, N., Barry, S., Weise, M. & Wolff-Holz, E. A data driven approach to support tailored clinical programs for biosimilar monoclonal antibodies. *Clin. Pharmacol. Ther.* **113**, 108–123 (2023).
17. Dou, Y.N., Grimstein, C., Mascaro, J. & Wang, J. Biomarkers for precision patient selection in cancer therapy approvals in the US, from 2011 to 2023. *Clin. Pharmacol. Ther.* **116**, 304–314 (2024).
18. Beckman, R.A., Antonijevic, Z., Kalamegham, R. & Chen, C. Adaptive design for a confirmatory basket trial in multiple tumor types based on a putative predictive biomarker. *Clin. Pharmacol. Ther.* **100**, 617–625 (2016).
19. Chelliah, V. *et al*. Quantitative systems pharmacology approaches for Immuno-oncology: adding virtual patients to the development paradigm. *Clin. Pharmacol. Ther.* **109**, 605–618 (2021).

nature publishing group

Biodistribution of ^{89}Zr-trastuzumab and PET Imaging of HER2-Positive Lesions in Patients With Metastatic Breast Cancer

EC Dijkers[1,2], TH Oude Munnink[3], JG Kosterink[1], AH Brouwers[2], PL Jager[2], JR de Jong[2], GA van Dongen[4], CP Schröder[3], MN Lub-de Hooge[1,2] and EG de Vries[3]

We performed a feasibility study to determine the optimal dosage and time of administration of the monoclonal antibody zirconium-89 (^{89}Zr)-trastuzumab to enable positron emission tomography (PET) imaging of human epidermal growth factor receptor 2 (HER2)-positive lesions. Fourteen patients with HER2-positive metastatic breast cancer received 37 MBq of ^{89}Zr-trastuzumab at one of three doses (10 or 50 mg for those who were trastuzumab-naive and 10 mg for those who were already on trastuzumab treatment). The patients underwent at least two PET scans between days 2 and 5. The results of the study showed that the best time for assessment of ^{89}Zr-trastuzumab uptake by tumors was 4–5 days after the injection. For optimal PET-scan results, trastuzumab-naive patients required a 50 mg dose of ^{89}Zr-trastuzumab, and patients already on trastuzumab treatment required a 10 mg dose. The accumulation of ^{89}Zr-trastuzumab in lesions allowed PET imaging of most of the known lesions and some that had been undetected earlier. The relative uptake values (RUVs) (mean ± SEM) were 12.8 ± 5.8, 4.1 ± 1.6, and 3.5 ± 4.2 in liver, bone, and brain lesions, respectively, and 5.9 ± 2.4, 2.8 ± 0.7, 4.0 ± 0.7, and 0.20 ± 0.1 in normal liver, spleen, kidneys, and brain tissue, respectively. PET scanning after administration of ^{89}Zr-trastuzumab at appropriate doses allows visualization and quantification of uptake in HER2-positive lesions in patients with metastatic breast cancer.

Human epidermal growth factor receptor 2 (HER2) is involved in cell survival, cell proliferation, cell maturation, metastasis, and angiogenesis, as well as exerting antiapoptotic effects.[1] Targeting of HER2 with the monoclonal antibody trastuzumab (Herceptin) is a well-established therapeutic strategy in the metastasized and adjuvant setting, and it has positively affected the prognosis of patients with breast cancer characterized by HER2-protein overexpression and/or amplification.[2,3]

HER2 status is routinely determined using immunohistochemistry or fluorescence *in situ* hybridization at the time of diagnosis of the primary tumor. However, there are data indicating that the HER2 status of a tumor can vary during the course of the disease.[4] In addition, there can be a discordance in HER2 expression across tumor lesions in the same patient.[5–7] Therefore, clinical guidelines encourage the use of repeated biopsies during the course of the disease.[8,9] Physicians and patients are nevertheless frequently reluctant to use this invasive technique; in addition, technical problems can arise when lesions are poorly accessible.[10]

Noninvasive HER2 imaging using single-photon emission computed tomography (SPECT) and positron emission tomography (PET) could be a strategy to determine HER2 expression and localization of HER2-overexpressing tumor lesions, including inaccessible distant metastases. This strategy, which could potentially guide HER2-targeted therapies, led to the development of ^{111}In-trastuzumab. Using this SPECT tracer, we have shown HER2-specific uptake in patients with HER2-positive metastatic breast cancer. ^{111}In-trastuzumab imaging discovered new HER2-positive lesions in 13 of 15 patients and was therefore considered to be of potential value as a clinical diagnostic tool in metastatic disease.[11] It was only after our ^{111}In-trastuzumab clinical study was completed that the long-lived PET isotope zirconium-89 (^{89}Zr) became available for clinical immunoPET imaging with ^{89}Zr-labeled antibodies.[12] For immunoPET

[1]Department of Hospital and Clinical Pharmacy, University of Groningen, Groningen, The Netherlands; [2]Department of Nuclear Medicine and Molecular Imaging, University of Groningen, Groningen, The Netherlands; [3]Department of Medical Oncology, University Medical Center Groningen, University of Groningen, Groningen, The Netherlands; [4]Department of Otolaryngology/Head and Neck Surgery, VU University Medical Center, Amsterdam, The Netherlands. Correspondence: EG de Vries (e.g.e.de.vries@int.umcg.nl)

Received 24 November 2009; accepted 21 January 2010; advance online publication 31 March 2010. doi:10.1038/clpt.2010.12

imaging, positron-emitting radiometals such as ^{89}Zr have an advantage over radiohalogens such as ^{124}I because they are residualizing and are therefore retained within the target cell after internalization and intracellular degradation of the tracer. This results in higher uptake in the tumor when an internalized antibody such as trastuzumab is used.[7] Of the positron-emitting radiometals, ^{89}Zr has the longest and therefore most favorable half-life (78.4 h), allowing antibody imaging up to 7 days after the injection. Preclinical evaluation of ^{89}Zr-trastuzumab showed that it displays superior image quality as compared to ^{111}In-trastuzumab, given the high spatial resolution and sensitivity of PET, although the uptake levels of ^{89}Zr-trastuzumab and ^{111}In-trastuzumab in the tumors were equivalent.[13] In addition, PET imaging has the advantage of allowing straightforward data quantification and whole-body 3D imaging. In view of these advantages, we performed this clinical study using ^{89}Zr-trastuzumab PET.

In this clinical study, we evaluated the optimal conditions for the administration of ^{89}Zr-trastuzumab to enable PET visualization and quantification of HER2-positive lesions in patients with HER2-positive metastatic breast cancer. We did this by comparing three relevant doses at early and late imaging times.

RESULTS

Patient characteristics

Between March 2006 and December 2008, 14 patients were enrolled in the study. Patient characteristics are presented in Table 1. The patients received 38.4 ± 1.6 MBq ^{89}Zr-trastuzumab. No infusion-related reactions or adverse events were noticed during the study. **Supplementary Table S1** online provides study details for individual patients, including the trastuzumab dose calculated for patients already on trastuzumab, the number of scans carried out and their timing, and the biodistribution of ^{89}Zr-trastuzumab and its uptake in lesions.

Trastuzumab dose for ^{89}Zr-trastuzumab PET imaging

The 10 mg trastuzumab dose in cohort 1 (n = 2) resulted in a relatively high uptake in the liver and a pronounced intestinal excretion of ^{89}Zr-trastuzumab. As a result, the amount of ^{89}Zr-trastuzumab in the blood pool was limited in these trastuzumab-naive patients (Figure 1a). Probably because rapid hepatic clearance prohibited optimal uptake of ^{89}Zr-trastuzumab in the tumors, the lesions could be visualized in only one of these two patients. We concluded that 10 mg trastuzumab was not sufficient for adequate imaging in trastuzumab-naive patients, and this cohort was therefore closed.

The 50 mg trastuzumab dose in cohort 2 (n = 5) resulted in less uptake in the liver and lower subsequent intestinal excretion as compared with patients in cohort 1. ^{89}Zr-trastuzumab was present in the blood pool during the scan sequence in all five patients (Figure 1b), indicating retarded blood pool clearance. Visual analysis revealed good tumor/nontumor ratios in this cohort. Therefore, 50 mg trastuzumab was considered to have a favorable biodistribution and to be adequate for HER2 PET imaging in trastuzumab-naive patients.

In the patients in cohort 3, who were already on trastuzumab (n = 7), a 10 mg dose of trastuzumab resulted in minimal intestinal excretion and slow ^{89}Zr-trastuzumab blood clearance (Figure 1c); 10 mg was therefore considered an adequate dose for patients already on trastuzumab therapy.

Dose-dependent blood clearance of ^{89}Zr-trastuzumab seen in the visual analysis was confirmed by quantitative analysis of ^{89}Zr-trastuzumab presence in the cardiac blood pool. Figure 1d shows the quantitative PET analysis of the relative blood pool activity levels of ^{89}Zr-trastuzumab as fitted curves for 5 days after injection in all three cohorts. The curve is lowest for cohort 1 and shows little change during the 5-day period, indicating rapid

Table 1 Patient characteristics

Characteristic	
Number of participants	14
Age (years)	
Median	48
Range	32–74
Body weight (kg)	
Median	72
Range	47–97
^{89}Zr-trastuzumab dose (n)	
10 mg ^{89}Zr-trastuzumab	2
50 mg ^{89}Zr-trastuzumab	5
10 mg ^{89}Zr-trastuzumab + trastuzumab therapy	7

^{89}Zr, zirconium-89.

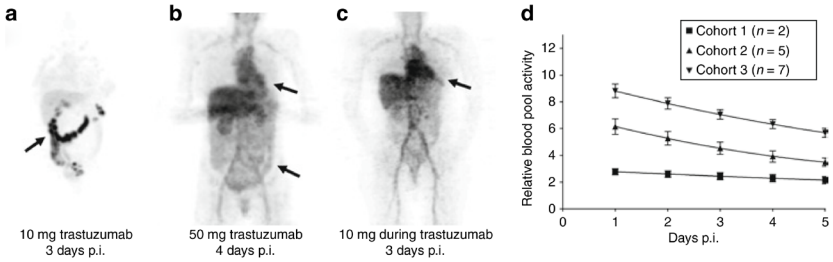

Figure 1 Dose-dependent ^{89}Zr-trastuzumab biodistribution. (**a–c**) Dose-dependent biodistribution and blood clearance of ^{89}Zr-trastuzumab. Radioactivity in the blood pool and intestinal excretion are indicated by arrows. (**d**) The "relative blood pool activity" represents the amount of ^{89}Zr-trastuzumab present in the blood pool relative to the total amount of ^{89}Zr-trastuzumab present during 5 days after the injection. ^{89}Zr, zirconium-89.

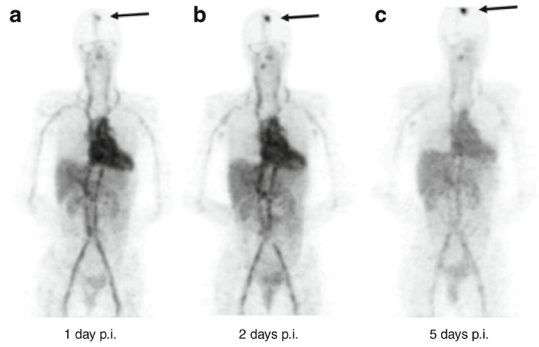

Figure 2 ^{89}Zr-trastuzumab biodistribution in time. (**a–c**) Three ^{89}Zr-trastuzumab scans of a patient already on trastuzumab treatment (cohort 3) show the increase over time in the tumor/nontumor ratio as regards uptake of the tracer. Arrow indicates ^{89}Zr-trastuzumab uptake in the only lesion. ^{89}Zr, zirconium-89.

blood pool clearance within the first 24 h. Patients in cohorts 2 and 3 show a much higher relative blood pool activity, indicating slow clearance of ^{89}Zr-trastuzumab from the blood pool.

Interval between tracer injection and PET scan

Except in the 10-mg dose group (cohort 1), extensive ^{89}Zr-trastuzumab activity was still present in the blood pool 1–2 days after the injection, even while uptake was observed in liver, spleen, and kidneys. At 4–5 days after the injection, ^{89}Zr-trastuzumab activity in the blood pool was lower, and uptake in tumors had increased. This is illustrated by means of the scans obtained from a patient already on trastuzumab treatment (**Figure 2a–c**). This representative patient showed a slight decrease in blood pool tracer activity and marked ^{89}Zr-trastuzumab accumulation in the brain metastasis over time.

Scans performed at day 6 or 7 after the injection yielded decreased image quality because of insufficient counting statistics. The optimal time for the scan represents a balance between good tumor/nontumor ratios and sufficient radioactive signal. The best time for assessing uptake of ^{89}Zr-trastuzumab in tumor lesions was found to be 4–5 days after the injection of 37 MBq ^{89}Zr-trastuzumab.

Visual analysis and quantification of ^{89}Zr-trastuzumab uptake

At visual examination, the spatial resolution and signal/noise ratios of the ^{89}Zr-trastuzumab PET scans were superior to those from our previous ^{111}In-trastuzumab SPECT study.[11]

Visual analysis of the PET scans revealed ^{89}Zr-trastuzumab biodistribution to liver, spleen, and kidney. This is in accordance with what was expected for these well-perfused organs. The ^{89}Zr-trastuzumab uptake in other nontumor tissues (e.g., lung, muscle, bone, and brain) was low.

In cohort 1, one of the two trastuzumab-naive patients showed accumulation of ^{89}Zr-trastuzumab in skin and liver metastases.

In both cohort 2 and cohort 3, the majority of the lesions previously identified in the patients by computed tomography (CT), magnetic resonance imaging (MRI), or bone scans could

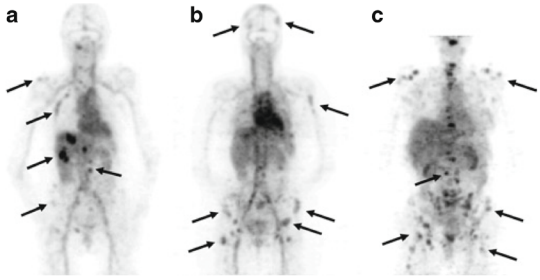

Figure 3 Examples of ^{89}Zr-trastuzumab uptake 5 days after the injection. (**a**) A patient with liver and bone metastases, and (**b** and **c**) two patients with multiple bone metastases. A number of lesions have been specifically indicated by arrows. See **Supplementary Movies S1 and S2** online for rotating 3D projections of **a** and **c**. ^{89}Zr, zirconium-89.

also be seen on the ^{89}Zr-trastuzumab PET scan. Visually, no difference was evident between cohorts 2 and 3 with respect to the uptake of ^{89}Zr-trastuzumab in tumor lesions. We anticipated that, because cohorts 2 and 3 would have sufficient ^{89}Zr-trastuzumab in the circulation (in contrast to cohort 1), there would be sufficient ^{89}Zr-trastuzumab available for accumulation in the tumors in these two cohorts. In addition, because the relative uptake values (RUVs) for these two cohorts were very similar (as shown in **Supplementary Table S1** online), the cohorts' data pertaining to uptake of ^{89}Zr-trastuzumab in tumors were pooled (n = 12).

In 6 of these 12 patients, ^{89}Zr-trastuzumab PET did not detect all the known lesions.

Known liver lesions were visualized by ^{89}Zr-trastuzumab in four of seven patients. No uptake of ^{89}Zr-trastuzumab took place in liver lesions in two of the patients in cohort 2 and one patient in cohort 3. **Figure 3a**, an image from a representative patient with liver and bone metastases as revealed by CT and bone scan, shows a clear distinction between normal and pathological ^{89}Zr-trastuzumab uptake in the liver on the day-5 scan. ^{89}Zr-trastuzumab PET did not reveal any liver lesions.

At the time of the tracer injection, one of the patients with known liver metastases had been receiving trastuzumab treatment for 2 months. A CT scan performed directly after the PET scan (following ^{89}Zr-trastuzumab administration) showed a partial tumor response. This response, probably associated with tumor cell apoptosis and receptor occupation and/or internalization, might explain the negative results of the ^{89}Zr-trastuzumab PET scan.

Multiple bone lesions, noted on bone scans, CT, or MRI, were visualized by ^{89}Zr-trastuzumab PET in seven of nine patients. The two patients in whom the bone lesions did not show uptake of ^{89}Zr-trastuzumab were in cohort 3. Representative examples of ^{89}Zr-trastuzumab uptake in bone lesions are shown in **Figure 3a–c** (**Figure 3a and c** are also available online as rotating 3D projections; see **Supplementary Movies S1 and S2** online). The various bone lesions in the two patients are shown in the ^{89}Zr-trastuzumab PET scans and were in good agreement with ^{99m}Tc-HDP bone scans. **Figure 4a** shows the ^{89}Zr-trastuzumab uptake in a vertebral metastasis detected earlier

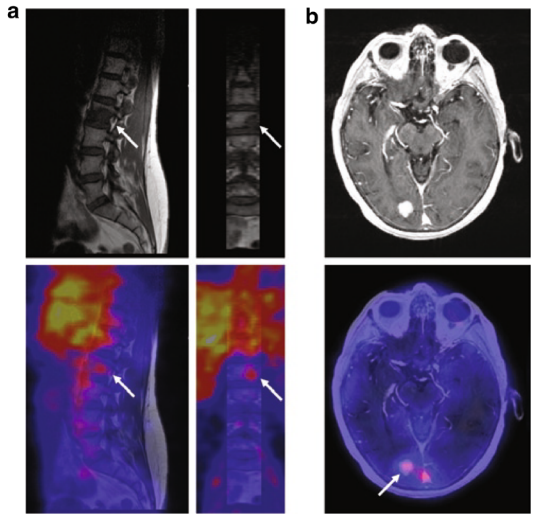

Figure 4 Examples of fusion images from HER2 PET and MRI scans. (**a**) In a vertebral metastasis seen on MRI but unapproachable for biopsy, HER2 status was revealed by ^{89}Zr-trastuzumab uptake on PET imaging. (**b**) Example of HER2-positive brain lesion undetected by conventional scans, revealed by ^{89}Zr-trastuzumab PET imaging, and subsequently confirmed by MRI. Arrows indicate lesions. HER2, human epidermal growth factor receptor 2; MRI, magnetic resonance imaging; PET, positron emission tomography; ^{89}Zr, zirconium-89.

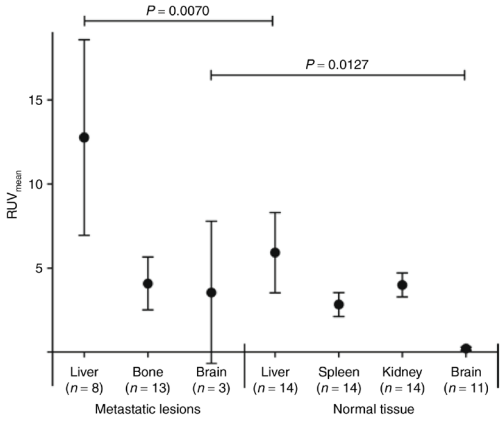

Figure 5 Relative uptake values (RUVs) are quantified for metastatic lesions and for normal liver, spleen, kidney, and brain. RUVs shown here are from the later-time scans.

by MRI. Bone lesions that had not been detected by other scans were discovered by PET scan in one patient in cohort 2.

In three patients, brain metastases were visualized by ^{89}Zr-trastuzumab PET. In one patient (from cohort 2) with two brain lesions as seen on MRI, the PET scan showed ^{89}Zr-trastuzumab accumulation in one of the metastases (measuring 2.0 × 1.6 cm on MRI); the other tumor lesion (measuring 0.5 × 0.5 cm on MRI) did not show up in the PET scan. In two other patients (one each in cohorts 2 and 3), ^{89}Zr-trastuzumab PET imaging revealed previously undetected brain metastases, both subsequently confirmed by MRI (**Figure 4b**). The smallest brain lesion revealed by ^{89}Zr-trastuzumab PET imaging measured 0.7 × 0.7 cm on MRI.

Uptake of ^{89}Zr-trastuzumab in metastatic lesions was seen in one of the three patients (all in cohort 3) with known lung metastases.

No lymph node metastases were detected during physical examination, CT, MRI, or ^{89}Zr-trastuzumab PET scans.

The uptake of ^{89}Zr-trastuzumab in metastatic lesions and normal tissue was quantified as RUV_{mean}. The uptake in metastatic lesions was also quantified as RUV_{max}; this showed an excellent correlation (R^2 = 0.974; slope 1.36) between RUV_{mean} and RUV_{max}, indicating a homogeneous uptake within the lesions. Liver lesions displayed the highest level of uptake (12.8 ± 5.8), higher than that of normal liver (5.9 ± 2.4, P = 0.0070) or that of any other normal tissue (**Figure 5**). Uptake in brain lesions was higher than in normal brain tissue (3.5 ± 4.2 vs. 0.20 ± 0.1, P = 0.0127), although there was a relatively large variation in uptake values between types of lesions. ^{89}Zr-trastuzumab RUV_{mean} in bone lesions was 4.1 ± 1.6. The uptake for normal bone was too low to be quantified. The RUV_{mean} of the only lung lesion was 4.3.

DISCUSSION

This first-in-human ^{89}Zr-trastuzumab HER2 PET imaging study showed excellent tumor uptake and visualization of HER2-positive metastatic liver, lung, bone, and even brain tumor lesions, when an adequate trastuzumab protein dose was administered. In trastuzumab-naive patients with HER2-positive metastatic breast cancer, 50 mg of trastuzumab was the dose that resulted in optimal biodistribution characteristics under the test conditions and proved adequate for ^{89}Zr-trastuzumab PET imaging. The 50-mg trastuzumab dose in naive patients is a good starting point for further optimization in future studies. In patients undergoing treatment with trastuzumab at the time of tracer injection, 10 mg trastuzumab was adequate for PET imaging. Higher doses of trastuzumab were not expected to improve ^{89}Zr-trastuzumab PET imaging; trastuzumab clearance was already minimal, and therefore a further increase in the dose of trastuzumab could induce target saturation. Quantification of the PET images confirmed the dose-dependency of trastuzumab clearance and revealed a significantly higher uptake in metastatic tumor lesions as compared to corresponding normal tissue. In this study, ^{89}Zr-trastuzumab allowed the researchers to distinguish between lesions with HER2 overexpression and those without. The exact amount of HER2 expression required for adequate imaging will have to be determined in a future biopsy-aligned study.

The rapid ^{89}Zr-trastuzumab clearance, as seen with a 10-mg dose administered to trastuzumab-naive patients in cohort 1, is in accordance with trastuzumab pharmacokinetic data from phase I studies.[14,15] After multiple doses at therapeutic concentrations, trastuzumab clearance has an average terminal half-life of 28.5 days at steady state.[16] However, when given as

a single dose of 10 or 50 mg, trastuzumab is known to have an average terminal half-life of 1.5 or 4.3 days, respectively.[14] This short-terminal half-life is probably too brief to allow adequate accumulation of the tracer in the tumors and subsequent imaging when 10 mg of the tracer is used in ^{89}Zr-trastuzumab-naive patients. This analysis is supported by the presence of ^{89}Zr in the intestinal tract in patients in cohort 1.

Dose-dependent pharmacokinetics has also been shown to hold good for the trastuzumab–DM1 antibody–drug conjugate and for the HER2 antibody pertuzumab.[17,18] The exact mechanisms underlying these dose-dependent pharmacokinetics of HER2-targeted antibodies are not known, but they probably involve rapid but saturable elimination of low doses from the first compartment of distribution, i.e., the circulation, during the first elimination phase. Elimination of trastuzumab is characterized by two phases; a first phase with a half-life of ~4 days, followed by a second phase that starts ~1 week after infusion, with a much longer half-life.[19] Saturable elimination in the first phase is probably caused by antibody catabolism followed by excretion of the catabolites. A second mechanism that can play a role in increasing ^{89}Zr-trastuzumab clearance in trastuzumab-naive patients is the presence of high plasma levels of extracellular domains shed by HER2.[16] After the binding of trastuzumab to these extracellular domains, this complex is cleared by the liver and excreted in the intestines.

The administered ^{89}Zr dose of 37 MBq proved to be sufficient for adequate imaging up to 5 days after the injection. Because of the balance between the relatively slow accumulation of trastuzumab in the tumors and the radioactive decay of ^{89}Zr, a suitable time for assessing ^{89}Zr-trastuzumab tumor uptake was found to be 4–5 days after the injection. The PET images produced with ^{89}Zr-trastuzumab showed high spatial resolution and good signal-to-noise ratio, resulting in an image quality unapproachable by our previous ^{111}In-trastuzumab SPECT scans.[11,20] As compared to the 75 MBq used in the only earlier clinical study with ^{89}Zr, the 37 MBq used in the present study resulted in a lower radiation dose to the patient while preserving image quality.[12] On the basis of the previous ^{111}In-trastuzumab study (after substituting nuclide properties) the ^{89}Zr-trastuzumab radiation dose was estimated at 18 mSv, comparable to two abdominal CT scans.[21]

Although our study was not designed for head-to-head comparison with conventional staging modalities or for assessing sensitivity and specificity, lesions with ^{89}Zr-trastuzumab uptake were generally in agreement with available data from CT, MRI, and bone scans. In approximately half the patients evaluated, PET scans showed no uptake of ^{89}Zr-trastuzumab in certain tumor lesions, although these lesions had previously been identified with conventional imaging. This may be attributable to variable HER2 expression in different lesions in the same patient,[4–7] although this cannot be stated with absolute certainty because no biopsies of those specific lesions were carried out. It is unlikely that in cohort 3 (patients on trastuzumab treatment) some of the tumor lesions had no uptake of ^{89}Zr-trastuzumab due to saturation, because lesions overall showed up very well in this cohort. Therefore, future studies to assess the sensitivity and specificity of HER2 PET imaging should compare the uptake of ^{89}Zr-trastuzumab in tumor lesions with the pathological HER2 status of these lesions, as seen from biopsies. The process of obtaining biopsy specimens will need to be carefully performed because tumor lesions may be difficult to access; an additional consideration is that undergoing more than one biopsy may be too burdensome to the patient.

Until additional information from these future studies becomes available, it will remain unclear whether nondetection of known lesions by ^{89}Zr-trastuzumab PET imaging occurs because of suboptimal imaging conditions (e.g., dosing and timing, lesion size, spatial resolution) or because the level of HER2 overexpression in these lesions has fallen below the limit detectable by PET.

The fact that we were able to visualize brain lesions was interesting, given that it is generally believed that trastuzumab has poor penetration of the brain.[22] This study shows that ^{89}Zr-trastuzumab can target brain lesions, with an 18-fold higher uptake in tumors than in normal brain tissue. This is probably because of a disruption of the blood–brain barrier at the site of the brain metastasis, and it supports the use of trastuzumab therapy in patients with HER2-positive breast cancer and brain metastases.

In addition to ^{89}Zr-trastuzumab and ^{111}In-trastuzumab, a few other tracers have been used for clinical HER2 imaging. The ^{99m}Tc-labeled anti-HER2 rat antibody ICR12 was administered to eight breast cancer patients in the early 1990s. This SPECT study suggested that ^{99m}Tc-ICR12 could be used for the imaging of HER2-positive disease, although no further clinical results involving this antibody have been made available.[23] Currently, clinical studies with ^{111}In- and ^{64}Cu-trastuzumab and with ^{68}Ga-trastuzumab F(ab′)$_2$ fragments are at the stage of patient recruitment.[24–26] These studies will give insight into the possibility of using shorter-lived isotopes (such as ^{64}Cu) for imaging with intact antibodies and will provide the first clinical results with the smaller HER2-directed F(ab′)$_2$ fragments. Generally, large intact monoclonal antibodies penetrate slowly but constantly into solid tumor tissue, ultimately resulting in higher accumulation in the tumor than is the case with small proteins; antibody fragments penetrate more swiftly into tumor tissue but show less uptake in the tumor because of more rapid clearance from the blood.[7]

If, in the future, other tracers prove to be more useful than ^{89}Zr-trastuzumab for HER2 PET imaging in patients, the choice of tracer might well depend on the purpose for which HER2 PET imaging is to be used. One can envision a role for HER2 PET imaging in improving diagnosis, staging (especially in clinical dilemmas such as when lesions are inaccessible for biopsy), guiding individual trastuzumab therapy, and early drug development of HER2-targeting agents.[7,27]

This feasibility-evaluation of biodistribution and imaging points to the need for further exploration of ^{89}Zr-trastuzumab HER2 PET imaging.

METHODS

Patients. In this prospective imaging feasibility study in female patients with metastatic breast cancer, the eligibility criteria were (i) proven HER2-positive tumor at diagnosis (as confirmed by immunohistochemistry or fluorescence *in situ* hybridization), (ii) at least one tumor lesion

in situ at the time of inclusion, and (iii) age ≥18 years. Available standard staging procedures with conventional imaging such as radiography, CT, MRI, and bone scans were used for comparison. No standard CT or MRI scans of the brain were performed, except when there were neurological symptoms or suspicion of brain metastases, or where ^{89}Zr-trastuzumab uptake in the brain was seen on the PET scan. Exclusion criteria were (i) pregnancy, (ii) uncontrolled concurrent illness, and (iii) treatment with antibodies other than trastuzumab.

The study was approved by the medical ethical committee of the University Medical Center Groningen, and written informed consent was obtained from all patients.

Tracer and protein dose. Clinical grade ^{89}Zr-trastuzumab was produced as described previously.[13] In short, reconstituted trastuzumab (Roche, Woerden, The Netherlands) was conjugated with tetrafluorophenol-*N*-succinyldesferal-Fe (VU University Medical Center, Amsterdam, The Netherlands), purified, and stored at −80 °C. Good manufacturing practice-produced ^{89}Zr-oxalate (IBA Molecular Benelux, Louvain-La-Neuve, Belgium) was used for radiolabeling the conjugate. Quality control was performed to ensure (radio)chemical purity (>95%), antigen-binding capacity (>80%), and stability.

Patients received 37 MBq (1 mCi) ^{89}Zr-trastuzumab intravenously and were monitored for 30 min after the injection to detect any infusion-related anaphylactic reactions or adverse events.

To determine the minimal required trastuzumab dose, three cohorts of ^{89}Zr-trastuzumab protein dose were used: 10 mg (cohort 1) and 50 mg (cohort 2) in those who were trastuzumab-naive and 10 mg (cohort 3) for those already on trastuzumab treatment. Each of these doses consisted of ^{89}Zr-trastuzumab (~1.5 mg), replenished with nonradioactive trastuzumab. Patients on trastuzumab treatment had been receiving up to 6 mg/kg and therefore might already have had a significant amount of trastuzumab in their systems at the time of tracer injection (as is shown in **Supplementary Table S1** online, the trastuzumab range was 130–675 mg).

We aimed to recruit a maximum of five to seven patients per cohort. Each cohort was evaluated after data from two patients became available. If this evaluation indicated that the trastuzumab dose was insufficient for adequate imaging, the cohort was closed.

PET imaging, biodistribution, and quantification. Each patient underwent at least one PET scan at an early time (1–3 days after injection) and one at a later time (4–7 days after injection).

Images were obtained using a Siemens Exact HR+ PET camera (Siemens AG, Munich, Germany). Acquisition was carried out in 3D mode from upper thigh to head, in seven or eight bed positions with 9–12 min of imaging (including 20–22% transmission time) per bed position. PET images were reconstructed using the ordered-subsets expectation maximization algorithm, with two iterations and eight subsets.

The biodistribution of (radiolabeled) antibodies is slow ($T_{½}$ of days). It was therefore expected that the biodistribution during the timeframe of the PET scan would not be a relevant factor. A single frame was acquired to obtain maximal counting statistics and the best image quality.

The PET scans were visually examined, and ^{89}Zr-trastuzumab distribution was assessed in accordance with the protocol for blood pool, liver, spleen, kidneys, bone marrow, and intestines. The number of metastases was determined.

Quantification of ^{89}Zr-trastuzumab distribution was performed using AMIDE software (version 0.9.1; Stanford University, Palo Alto, CA).[28] Instead of the frequently used standardized uptake value, we used a modified parameter, RUV, to provide a semiquantitative representation of the tissue-to-background ratio. RUV is related to the amount of tracer present in the body at the moment of scan acquisition, whereas standardized uptake value is related to the amount of tracer injected. RUV is independent of the rate of excretion of the ^{89}Zr-trastuzumab tracer and can therefore be used to quantify uptake for a period of days after the injection. For calculating RUV, we used the whole-body mean uptake (WB_{mean}) value based on the radioactivity within the field of view (rather than on the radioactivity within the region of interest, which is used in arriving at standardized uptake value). The RUV_{mean} was calculated as the ratio of mean tissue uptake to mean whole-body uptake for each scan:

$$RUV_{mean} = \frac{Tissue_{mean,scanX}}{WB_{mean,scanX}} = \frac{Tissue_{mean,scanX}}{A_{WB,scanX}/V_{WB,scanX}}$$

The mean tissue uptake ($Tissue_{mean}$) was determined by manually drawing a volume of interest in metastatic lesions and in normal tissues (heart, liver, spleen, kidneys, bone, and brain) and measuring the mean radioactivity in the volume of interest for all tumor lesions and tissues. The WB_{mean} was calculated by dividing total radioactivity in the field of view (A_{WB}) by the volume represented within the field of view (V_{WB}). The RUV_{max} was calculated by dividing the uptake in tissues in the most intense voxel of the volume of interest by WB_{mean}. The blood pool ^{89}Zr-trastuzumab activity was calculated for the first 5 days after injection by interpolating the volume of interest RUVs of each patient's cardiac blood pool into an exponential fitting model.

Statistics. Data are presented as means ± SD. Statistical analysis was performed using the nonparametric Mann–Whitney *U*-test (Graphpad Prism 5; Graphpad Software, La Jolla, CA). *P* values <0.05 were considered significant.

SUPPLEMENTARY MATERIAL is linked to the online version of the paper at http://www.nature.com/cpt

ACKNOWLEDGMENT

This study was supported by grant 2007-3739 from the Dutch Cancer Society.

CONFLICT OF INTEREST

The authors declared no conflict of interest.

1. Gross, M.E., Shazer, R.L. & Agus, D.B. Targeting the HER-kinase axis in cancer. *Semin. Oncol.* **31**, 9–20 (2004).
2. Slamon, D.J. *et al.* Use of chemotherapy plus a monoclonal antibody against HER2 for metastatic breast cancer that overexpresses HER2. *N. Engl. J. Med.* **344**, 783–792 (2001).
3. Piccart-Gebhart, M.J. *et al.* Trastuzumab after adjuvant chemotherapy in HER2-positive breast cancer. *N. Engl. J. Med.* **353**, 1659–1672 (2005).
4. Rasbridge, S.A. *et al.* The effects of chemotherapy on morphology, cellular proliferation, apoptosis and oncoprotein expression in primary breast carcinoma. *Br. J. Cancer* **70**, 335–341 (1994).
5. Solomayer, E.F. *et al.* Comparison of HER2 status between primary tumor and disseminated tumor cells in primary breast cancer patients. *Breast Cancer Res. Treat.* **98**, 179–184 (2006).
6. Wülfing, P. *et al.* HER2-positive circulating tumor cells indicate poor clinical outcome in stage I to III breast cancer patients. *Clin. Cancer Res.* **12**, 1715–1720 (2006).
7. Dijkers, E.C., de Vries, E.G., Kosterink, J.G., Brouwers, A.H. & Lub-de Hooge, M.N. Immunoscintigraphy as potential tool in the clinical evaluation of HER2/neu targeted therapy. *Curr. Pharm. Des.* **14**, 3348–3362 (2008).
8. National Comprehensive Cancer Network (NCCN) Clinical Practice Guidelines in Oncology—v.1.2009 <http://www.nccn.org/professionals/physician_gls/PDF/breast.pdf>.
9. Breast Cancer Treatment (PDQ®) <http://www.cancer.gov/cancertopics/pdq/treatment/breast/Healthprofessional/page8#Section_220>.
10. Lear-Kaul, K.C., Yoon, H.R., Kleinschmidt-DeMasters, B.K., McGavran, L. & Singh, M. Her-2/neu status in breast cancer metastases to the central nervous system. *Arch. Pathol. Lab. Med.* **127**, 1451–1457 (2003).
11. Perik, P.J. *et al.* Indium-111-labeled trastuzumab scintigraphy in patients with human epidermal growth factor receptor 2-positive metastatic breast cancer. *J. Clin. Oncol.* **24**, 2276–2282 (2006).
12. Börjesson, P.K. *et al.* Performance of immuno-positron emission tomography with zirconium-89-labeled chimeric monoclonal antibody U36 in the

detection of lymph node metastases in head and neck cancer patients. *Clin. Cancer Res.* **12**, 2133–2140 (2006).
13. Dijkers, E.C. *et al*. Development and characterization of clinical-grade ^{89}Zr-trastuzumab for HER2/neu immunoPET imaging. *J. Nucl. Med.* **50**, 974–981 (2009).
14. US Food and Drug Administration. FDA Clinical Review of BLA 98-0369: Herceptin Trastuzumab (rhuMAb HER2) <http://www.fda.gov/downloads/Drugs/DevelopmentApprovalProcess/HowDrugsareDevelopedandApproved/ApprovalApplications/TherapeuticBiologicApplications/ucm091373.pdf>.
15. Tokuda, Y. *et al*. Dose escalation and pharmacokinetic study of a humanized anti-HER2 monoclonal antibody in patients with HER2/neu-overexpressing metastatic breast cancer. *Br. J. Cancer* **81**, 1419–1425 (1999).
16. Bruno, R., Washington, C.B., Lu, J.F., Lieberman, G., Banken, L. & Klein, P. Population pharmacokinetics of trastuzumab in patients with HER2+ metastatic breast cancer. *Cancer Chemother. Pharmacol.* **56**, 361–369 (2005).
17. Beeram, M. *et al*. A phase I study of trastuzumab-DM1 (T-DM1), a first-in-class HER2 antibody-drug conjugate (ADC), in patients (pts) with advanced HER2+ breast cancer (BC) [abstr.]. *J. Clin. Oncol*. **26** (suppl.), 1028 (2008).
18. Agus, D.B. *et al*. Phase I clinical study of pertuzumab, a novel HER dimerization inhibitor, in patients with advanced cancer. *J. Clin. Oncol.* **23**, 2534–2543 (2005).
19. Baselga, J. *et al*. Phase II study of efficacy, safety, and pharmacokinetics of trastuzumab monotherapy administered on a 3-weekly schedule. *J. Clin. Oncol.* **23**, 2162–2171 (2005).
20. de Korte, M.A. *et al*. 111Indium-trastuzumab visualises myocardial human epidermal growth factor receptor 2 expression shortly after anthracycline treatment but not during heart failure: a clue to uncover the mechanisms of trastuzumab-related cardiotoxicity. *Eur. J. Cancer* **43**, 2046–2051 (2007).
21. Brenner, D.J. & Hall, E.J. Computed tomography--an increasing source of radiation exposure. *N. Engl. J. Med. 357*, 2277–2284 (2007).
22. Lin, N.U. & Winer, E.P. Brain metastases: the HER2 paradigm. *Clin. Cancer Res.* **13**, 1648–1655 (2007).
23. Allan, S.M. *et al*. Radioimmunolocalisation in breast cancer using the gene product of c-erbB2 as the target antigen. *Br. J. Cancer* **67**, 706–712 (1993).
24. PET Imaging With Cu-64 Labeled Trastuzumab in HER2^{+} Metastatic Breast Cancer (Cu-64 HER2^{+}). <http://clinicaltrials.gov/ct2/show/NCT00605397>.
25. Biodistribution and Dosimetry of Serial PET Imaging With Ga-68 Labeled F(ab') 2-Trastuzumab . <http://clinicaltrials.gov/ct2/show/NCT00613847>.
26. Breast Imaging Using Indium In 111 CHX-A DTPA Trastuzumab in Patients With Primary Cancer or Metastatic Cancer. <http://clinicaltrials.gov/ct2/show/NCT00474578>.
27. van Dongen, G.A., Visser, G.W., Lub-de Hooge, M.N., de Vries, E.G. & Perk, L.R. Immuno-PET: a navigator in monoclonal antibody development and applications. *Oncologist* **12**, 1379–1389 (2007).
28. Loening, A.M. & Gambhir, S.S. AMIDE: a free software tool for multimodality medical image analysis. *Mol. Imaging* **2**, 131–137 (2003).